LncRNA RAD51B-AS1 promotes the malignant biological behavior of ovarian cancer via upregulation of RAD51B

Xinyi Wei
Women's Reproductive Health Laboratory of Zhejiang Province, Women's Hospital, School of Medicine, Zhejiang University

Conghui Wang
Department of Gynecologic Oncology, Women's Hospital, School of Medicine, Zhejiang University

Sangsang Tang
Women's Reproductive Health Laboratory of Zhejiang Province, Women's Hospital, School of Medicine, Zhejiang University

Qian Yang
Department of Gynecologic Oncology, Women's Hospital, School of Medicine, Zhejiang University

Zhangjin Shen
Women's Reproductive Health Laboratory of Zhejiang Province, Women's Hospital, School of Medicine, Zhejiang University

Jiawei Zhu
Department of Gynecologic Oncology, Women's Hospital, School of Medicine, Zhejiang University

Xiaodong Cheng
Department of Gynecologic Oncology, Women's Hospital, School of Medicine, Zhejiang University

Xinyu Wang
Department of Gynecologic Oncology, Women's Hospital, School of Medicine, Zhejiang University

Xing Xie
Department of Gynecologic Oncology, Women's Hospital, School of Medicine, Zhejiang University

Junfen Xu
Department of Gynecologic Oncology, Women's Hospital, School of Medicine, Zhejiang University

Weiguo Lu (lbwg@zju.edu.cn)
Department of Gynecologic Oncology, Women's Hospital, School of Medicine, Zhejiang University

---

Research Article

Keywords: Ovarian cancer. LncRNA. Metastasis, Anoikis

Posted Date: February 10th, 2022

DOI: https://doi.org/10.21203/rs.3.rs-1333435/v1

Abstract

Background Ovarian cancer (OC) has the highest fatality rate amongst all gynecologic malignancies. Exploring new factors and pathways associated with development of ovarian cancer would help to identify new therapeutic targets. Long non-coding RNAs (lncRNAs) play indispensable roles in the process of the progression of OC.

Methods Reverse transcription-quantitative PCR (RT-qPCR) was performed to verify the expression of RAD51B-AS1 in cell lines and patients' tissues. Cellular proliferation, metastasis and apoptosis were detected using Cell Counting Kit-8(CCK-8), colony formation, Transwell and flow cytometry assays, respectively. Mouse xenograft models were established to detect tumorigenesis. RT-qPCR, western blotting and immunofluorescence experiments were conducted to explore the quantitative and positional relationship between RAD51B-AS1 and its host gene, RAD51B. Co-transfection rescue experiments were then performed to preliminarily explore its mechanism *in vivo and in vitro*.

Results RAD51B-AS1 was significantly upregulated in a highly metastatic human OC cell line and in OC tissues. RAD51B-AS1 significantly increased the proliferation and metastasis of OC cells, whilst also enhancing resistance to anoikis. Biogenetics prediction analysis revealed that the only target gene of RAD51B-AS1 was RAD51B. Subsequent gene function experiments revealed that RAD51B exerted the same biological effects as RAD51B-AS1. Rescue experiments demonstrated that the malignant biological behaviors promoted by RAD51B-AS1 overexpressing were partially or completely reversed by RAD51B silencing *in vitro and in vivo*.

Conclusion RAD51B-AS1 promoted the malignant biological behavior of OC, and the underlying mechanism of this action may be associated with the positive regulation of RAD51B expression. The present study revealed a potentially novel molecular mechanism underlying the development of OC. RAD51B-AS1 is expected to serve as a novel molecular biomarker for the diagnosis and prediction of a poor prognosis in OC, and as a potential therapeutic target for management of the disease.

1. Background

OC has the highest fatality rate amongst all gynecologic malignancies according to the latest data [1]. Due to the deep location of the ovary within the pelvic cavity, inconspicuous early symptoms and the lack of specific tumor markers, > 75% of patients with OC are diagnosed with late stage diseases (FIGO stages III-IV) in the first instance. Furthermore, patients often develop abdominal cavity spread and/or distant metastases [2-4]. Therefore, to understand the molecular mechanisms underlying the biological processes and development of OC, along with the elucidation of interventional measures are urgently required.

Long non coding RNAs consist of >200 nucleotides with limited or no protein-coding [5]. Currently, a growing number of lncRNAs have been reported to participate in the process of the progression of OC through a variety of pathways and molecular mechanisms [6-8]. Certain lncRNAs, such as MALAT1, ANRIL

and PTAR, have been identified as prognostic biomarkers [9-12]. However, the clinical significance and biological mechanisms of the overwhelming majority of lncRNAs remain unknown, highlighting the necessity for identification of novel lncRNAs as potential molecular markers for the diagnosis and treatment of OC.

The human OC cell line, HO8910PM, is a highly metastatic subline developed from the parental cell line, HO8910 [12-14]. Due to the different malignant capacities of these two cell lines, differences in lncRNA were detected using second-generation sequencing, with those that demonstrated significant differences being selected for RT-qPCR verification. These results aimed to identify novel lncRNAs associated with the development of OC. From these data, a novel lncRNA, ENST00000554679.1(RAD51B-AS1), was selected. Located on 14q24.1 and consisting of two exons, it was transcribed from the reverse strand of the RAD51B gene. To the best of our knowledge, the present study is the first to investigate the role and mechanism of lncRNA RAD51B-AS1 in OC development. The results of the current study may assist in the elucidation of potential diagnostic or therapeutic OC biomarkers.

2. Materials And Methods

2.1. Patients and tissue samples

49 samples of OC patients and 9 samples of ovarian benign tumor patients who performed surgery for the first time, without any radiotherapy, chemotherapy or neoadjuvant chemotherapy before surgery. Patient information is shown in Table S1. Exclusion criteria: patients with other malignant tumors or severe complicated diseases were excluded. The Ethics Committee of the Women's Hospital, school of medicine, Zhejiang University approved this study (granted number: IRB-20210147-R), and the participants were all provided informed consent.

2.2.Cell lines and cell culture.

The human ovarian cancer cell lines (HO8910 and HO8910-PM) were provided by the Women's Hospital, school of medicine, Zhejiang University, where they were tested and authenticated. All cells were cultured in RPMI 1640 (BI, Israel) medium containing 10% fetal bovine serum (FBS) in a 5% CO_2 humidified incubator at 37°C.

2.3.RNA sequencing analysis.

Total RNAs of HO8910 and HO8910PM cells were prepared by Trizol Reagent (Invitrogen, USA). RNA quality was evaluated by Agilent 2200(Agilent, USA). And high-quality RNA was used for RNA sequencing. Firstly, the rRNA was removed and then RNA was fragmented to about 200 nucleotides lengths. Secondly, complementary DNA (cDNA) was synthesized and purified. Thirdly, the ends of the cDNA were repaired and the primers were added for PCR amplification and purification. Finally, after quality inspected, libraries were sequenced by illumine Hiseq Platform (RiboBio CO., LTD,China).

2.4. RNA extraction and RT-qPCR

Total RNA was extracted by TRIzol reagent. The nuclear and cytoplasmic fractions were isolated by PARIS Kit RNA Isolation System (Invitrogen, Thermo Fisher Scientific). PrimeScript RT reagent Kit with gDNA Eraser (Takara Bio Inc.) were used for synthesizing cDNA, and RT-qPCR was performed through TB Green Premix Ex Taq (Takara Bio Inc.). Primers' sequences are provided in Table S2. Statistical analyses of the results were performed using the $2^{-\Delta\Delta CT}$ relative quantification method.

2.5. Northern blotting

Probes were prepared and digoxigenin-labeled by Sangon Biotech Co., Ltd. (Shanghai, China), whose sequences were shown in Table S3. Afterwards, 15 μg RNA was separated in 1% formaldehyde denatured gel after electrophoresis under the statement of 25 V constant pressure and low temperature overnight and subsequently transferred to HyBond N+ membrane by the upward capillary transfer method for 20 h. The membrane was prehybridized in a hybrid furnace at 50°C for 2 h and hybridized overnight in a 50°C hybridization apparatus. Following that, film was blocked for 1h and then reacted in antibody solution for 30 min. The final step is X-ray film exposure and records of results in the darkroom.

2.6. Transfection of siRNA and lentiviral vectors into ovarian cancer cells

SiRNAs purchased from GenePharm (Shanghai, China) were used to knock down RAD51B-AS1 or RAD51B, and efficiency had been evaluated by RT-qPCR. The sequences are represented in Table S4. Additionally, for the ectopic expression of RAD51B-AS1, the lentiviruses encoding the RAD51-AS1 sequence and the negative control lentiviruses (LV-RAD51B-AS1 and LV-NC, respectively, GeneChem, Shanghai, China) were infected into HO8910 cells. After 72 hours of infection, the cells were selected by complete culture medium containing 2 μg/mL puromycin.

2.7. CCK-8 assay

Cell proliferation was assessed by the CCK-8 assay (Dojindo Laboratories, Japan). The cells were seeded at 5×10^3 cells/well into 96-well plates. CCK-8 solution (10 μL) was added to each well at hours 0h, 24h, 48h, 72h and 96h post transfection. After incubation at 37°C for 2 hours, the absorbance at 450 nm was measured by a microplate reader (SkanIt RE for Varioskan Flash 2.4.3).

2.8. Plate colony formation assay and soft-agar colony formation assay

For plate colony formation assays, 500 cells per well were resuspended and added to six-well plates and incubated at 37 °C for 2 weeks. For soft-agar colony formation assays, 5000 cells per well were resuspended by complete culture medium containing 0.3% agarose, and then added to six-well plates already solidified by the laid medium containing 0.5% agarose, and incubated for 3 weeks. Colonies were fixed and stained with 0.1% crystal violet for 20 min. Cell colonies(>50 cells) were counted and analyzed per well.

2.9. Transwell migration and invasion assay

Cell migration and invasion assays were conducted by 24-well transwell plates (8 μm pore, Corning Costar, USA). The transwell filter inserts were coated with (invasion) or without (migration) Matrigel (BD Biosciences, 1:12 diluted). 3× 10^5 cells (invasion) or 2× 10^5 cells (migration) suspended in 200μL OPTI-MEM were added to the upper chamber, and 500μL high concentration medium containing 18%FBS was added to the lower chamber. Air bubbles should be avoided between the upper and lower chambers. After incubated for 24h, the cells which traversed the bottom of the upper chamber were fixed in 0.5% crystal violet solution for 20 min. And cells remaining in upper chamber were removed by cotton swabs. Images were captured and number of cells were counted per field.

2.10. Establishment of anoikis model

Adherent ovarian cancer cells were digested with 0.25% trypsin and added into a six-well plate with ultra-low attachment surface (polystyrene, non-pyrogenic) purchased from Corning, with about 2.5× 10^5 cells each well. Under these conditions, and the morphology and growth of the suspended cells were observed by microscope. The culture medium was changed about once 2 or 3 days depending on the state of the cells (medium changing method: after centrifugation at 800rpm for 3min, supernatant was discarded and cells were resuspended by fresh complete medium and then added to a new culture plate with ultra-low attachment surface).

2.11. Flow cytometric analysis of apoptosis

Adherent cells were cultured in serum-free medium to induce apoptosis and harvested 72 hours after transfection. Both cells digested with 400 μl of accutase (Invitrogen) and the supernatant were collected into a 15-ml collection tube. Suspended cells and their medium were collected, too. The samples were centrifuged at 1000 rpm for 5 min, and the precipitate was collected and washed by PBS twice. For apoptosis analysis, the cells were stained by an Annexin V-FITC/ propidium iodide (PI) Apoptosis Kit (MULTI SCIENCES, China). Thereafter, the cell apoptosis ratio was measured by a BD FACSVerse.

2.12. RNA fluorescence in-situ hybridization (FISH) and immunofluorescence assay

FISH probes targeting for RAD51B-AS1 were purchased from RiboBio CO., LTD (China). Briefly, HO8910 cells were grown on 4-chamber glass bottom dish (Cellvis, USA), fixed in a 4% formaldehyde solution for 30 minutes at room temperature, permeabilized in PBS containing 0.5% Triton X-100 for 5 minutes at 4°C, and then prehybridized at 37°C for 1 hour. Hybridization was conducted with FISH probes overnight at 37°C in the dark. If immunofluorescence assay was followed, cells were then blocked with 3% BSA for 1 hour. Then cells were incubated with primary antibody anti-RAD51B (Santa cruz) at 4°C overnight and secondary antibody FITC labeled anti-mouse(multisciences) at room temperature for 1 h. After the cells were gradually washed, DAPI was counterstained to visualize the cell nucleus. Finally, the dish was observed by confocal laser scanning microscopy (Olympus).

2.13. Western blotting

Firstly, cell protein lysates were separated in 10% SDS-PAGE gel, and then transferred to polyvinylidene difluoride membrane. Secondly, western blotting analysis was carried out with anti-RAD51B (Santa cruz), anti-Bcl-2(Santa cruz) antibodies. Anti-β-ACTIN antibody (Fdbio science) was used as an internal control. Thirdly, the membrane was washed and subsequently incubated with horseradish peroxidase-conjugated secondary antibodies (Cell Signaling Technology, USA). Finally, complexes were visualized with Fdbio-Dura Enhanced Chemiluminescence kit and the expression levels of proteins were assessed by Image J.

2.14. Mouse xenograft assay

An in vivo model of ovarian cancer was established by subcutaneously injecting 3-week-old female BALB/c nude mice (Silaike Experiment Animal Co., Ltd., Shanghai, China) with a rate of 5×10^6 HO8910 cells stably overexpressed RAD51B-AS1 per mouse (12 mice) and same number lentivirus infected negative control cells suspended in PBS (6 mice). After 1 week, tumors were formed in both groups of nude mice, the experimental group of LV-RAD51B-AS1 nude mice were randomly divided into two groups on average, one group was injected with si-RAD51B intratumorally every 3 days, the other group of nude mice and the control group of LV-NC nude mice were injected with the same amount of Si-NC every 3 days to control variables. The tumor volumes of the mice were measured every week and calculated by the following formula: tumor volume [mm^3] = 0.5 × Length × $Width^2$). After 5 weeks, nude mice were sacrificed, and the subcutaneous implanted tumors lesions were excised, weighed, measured and photographed. The half of the tumor tissues were used for RNA extraction and the other half were used for immunohistochemical staining. This experiment was carried out in accordance with the National Institutes of Health Guide for the Care and Use of Laboratory Animals and approved by the China Medical University Animal Care and Use Committee (Approval number: IACUC-20200506-07).

2.15. Immunohistochemistry (IHC) analysis

Tissue samples were fixed with 4% paraformaldehyde. In good fixed state, they were pruned, dehydrated, embedded, sliced, stained and sealed in strict accordance with pathological experiment detection standard operating procedure. Finally, the qualified samples were examined under microscopy. IHC analysis was performed with anti-RAD51B (Huabio), anti-Bcl-2(Abcam), anti-Ki-67(Abcam) antibodies.

2.16. Statistical analysis

SPSS 24 and Graphpad Prism 8 were used for all statistical analysis. Student's T test was used for comparison of data with normal distribution and homogeneity of variance, while Welch's Correction's unpaired T test was used for comparison of data with normal distribution but uneven variance. Nonparametric Mann-Whitney test was used for non-normal distribution data. Kaplan-Meier method was introduced for survival analysis. $P < 0.05$ indicated the significant difference.

3. Results

3.1. Identification and characterization of RAD51B-AS1

The lncRNA expression profiles of the ovarian carcinoma cell line, HO8910, and the derived cell line, HO8910PM, which has a higher malignancy than HO8910, were analyzed using high-throughput sequencing analysis (Figure 1A). The top 16 differentially expressed lncRNAs [$\log_2$(fold change)>2.5 or <-2.5, P<0.05] were selected for further validation (Table 1). Among those selected, ENST00000554679.1 (RAD51B-AS1) was determined to be the most significantly upregulated lncRNA following RT-qPCR (Figure 1B). RAD51B-AS1 is 537 bp in length, and was confirmed in the present study via northern blotting (Figure 1C). It was predominately located in the nucleus, as verified by subcellular fractionation followed by expression analysis (Figure 1D), and FISH analysis (Figure 1E). The current study then assessed RAD51B-AS1 expression in 49 serous ovarian carcinoma tissues and 9 benign tumors, revealing a remarkably increase in the expression of RAD51B-AS1 in cancer samples (Figure 1F).

Table 1. The function of lncRNAs expressed differentially between HO8910PM and HO8910

Name of lncRNAs	The expression level in HO8910PM	Function
NR_045196.2 (SNHG18)	Low	SNHG18 acts as a tumor suppressor and a diagnostic indicator in hepatocellular Carcinoma[15]；SNHG18 promotes glioma cell motility via disruption of α-Enolase nucleocytoplasmic transport[16]；SNHG18 indicates poor prognosis in Multiple Myeloma[17]；SNHG18 drives the growth and metastasis of non-small cell lung cancer[18]
ENST00000568391.1	High	Not reported
ENST00000607026.1	High	Not reported
NR_126480.1 (SALRNA1)	High	SALRNA1:A senescence-associated lncRNA can delay senescence[19]；a new therapeutic target to limit the irreversible apoptosis of lung epithelial cells in COPD patients[20].
ENST00000414885.1	High	Not reported
NR_110574.1	High	Not reported
NR_046837.1	High	Not reported
NR_125949.1	High	Not reported
NR_135108.1	High	Not reported
NR_125948.1	High	Not reported
NR_126420.1	High	Not reported
ENST00000557197.1	High	Not reported
ENST00000604215.1	High	Not reported
ENST00000599208.1	High	Not reported
ENST00000554679.1	High	Not reported
NR_027412.1 (LINC00910)	Low	LINC00910 is hypermethylated and highly expressed in gastric cancer[21].

3.2. lncRNA RAD51B-AS1 enhances growth, metastasis and anoikis resistance in OC cells

To clarify the biological functional roles of RAD51B-AS1 in malignant OC cells, knockdown and overexpression experiments were conducted. RAD51B-AS1 was knocked-down using two siRNAs transfected into HO8910PM cell lines. These were selected due to their relatively higher expression of lncRNA RAD51B-AS1. The knockdown experiments demonstrated a high knockdown efficiency (Figure 2A). In addition, an RAD51B-AS1 overexpression lentivirus was infected into HO8910 ovarian cells, which

possess lower levels of RAD51B-AS1, to establish a stably overexpressed RAD51B-AS1 cell line. The efficiency of this experiment was also demonstrated (Figure 2B). CCK-8 assays revealed that the proliferation of cells was significantly attenuated after the depletion of endogenous RAD51B-AS1 when compared with the negative control group (Figure 2C). Furthermore, proliferation was considerably increased following RAD51B-AS1 overexpression (Figure 2D). Similar trends were demonstrated in colony-formation and survival assays following RAD51B-AS1 knockdown (Figure 2E) and overexpression (Figure 2F). In the RAD51B-AS1 knockdown group, the migration and invasion of cells was markedly decreased compared with the control group (Figure 2G), while the RAD51B-AS1 overexpression group significantly increased these effects (Figure 2H). We revealed that RAD51B-AS1 can promote the anoikis resistance of OC cells. The highly metastatic cell line HO8910PM demonstrated stronger anoikis resistance when compared with its parent cell line HO8910 (Figure S1A). This may be a mechanism by which stronger metastasis conferred. To investigate this hypothesis, functional assays regarding the anoikis resistance of RAD51B-AS1 were carried out. The results revealed that RAD51B-AS1 knockdown significantly increased the apoptotic rate of OC cells when cells were attached and detached (Figure 2I), while overexpression of RAD51B-AS1 significantly reduced these effects (Figure 2J). This indicated that anoikis resistance was significantly weakened after RAD51B-AS1 silencing and enhanced after RAD51B-AS1 overexpression. In the soft agar assay, the anchor-independent growth of OC cells was significantly reduced after RAD51B-AS1 knockdown (Figure S1B) and increased after RAD51B-AS1 overexpression (Figure S1C). As Bcl-2 is an anti-anoikis gene, its protein expression levels were reduced following RAD51B-AS1 downregulation (Figure 2K), while RAD51B-AS1 overexpression resulted in increased expression (Figure 2L). Furthermore, adherent HO8910 cells were compared with the same generation of HO8910 cells that were suspended for 24 and 48 h. The results revealed that intracellular RNA levels of lncRNA RAD51B-AS1 were significantly increased after suspension was induced (Figure 2M), indicating that RAD51B-AS1 contributed to the anoikis resistance of OC.

3.3. RAD51B-AS1 positively regulates RAD51B

Biogenetics prediction analysis of the downstream target genes of lncRNA RAD51B-AS1 was conducted. Since RAD51B-AS1 was mainly located in the nucleus, the ways in which it regulates its target genes were primarily divided into cis and trans regulation. Potential cis-regulated lncRNA target genes were obtained by integrating the differentially expressed lncRNAs with their adjacent (10 kb) mRNA data. For the prediction of trans regulation, sequences of differentially expressed lncRNAs and mRNAs were first extracted, after which BLAST software was used for primary screening (e<1E-5) and RNAPlex software was used for secondary screening to identify the possible target genes of lncRNA. As demonstrated in Tables S5 and S6, the only identified target gene was RAD51B.

FISH assays revealed that RAD51B-AS1 and RAD51B were both located in the nucleus in close proximity to each other and with the stable overexpression of RAD51B-AS1, the fluorescence intensity of RAD51B also increased (Figure 3A). Data from 49 cases of OC were subsequently analyzed, and there was clear evidence of a positive linear correlation between RAD51B-AS1 and RAD51B (Figure 3B). To verify that RAD51B was the target gene of RAD51B-AS1, RT-qPCR and western blotting assays were carried out. Due

to the position of RAD51B-AS1 corresponding to the intron of RAD51B, the two transfected siRNAs did not have any effect on RAD51B mRNA levels (Figure S2A). RAD51B-AS1 knockdown and overexpression markedly decreased and elevated RAD51B mRNA expression levels, respectively (Figure 3C and 3D). Additionally, western blotting analyses revealed that RAD51B protein levels were markedly different (Figure 3E and 3F), which was consistent with mRNA levels in dysregulated RAD51B-AS cell lines. Thus, the results suggested that RAD51B-AS1 may regulate RAD51B expression at the transcriptional and translational level. It was hypothesized that RAD51B-AS may facilitate OC progression by increasing RAD51B expression.

3.4. RAD51B promotes the malignant biological behavior of OC

RAD51B was markedly upregulated in OC tissues (Figure 4A). Based on the Kaplan-Meier Plotter online database, survival plots revealed that the patients with higher RAD51B expression levels had a lower progression-free survival (Figure. 4B) and overall survival (Figure 4C). To determine and research the potential regulatory role of RAD51B in the malignant biological behavior of OC, RAD51B expression was downregulated in HO8910PM cells by transfecting with si-RAD51B, which simultaneously reduced the expression of the anti-apoptotic protein Bcl-2 (Figure 4D). Subsequently, CCK-8 (Figure 4E) and colony formation (Figure 4F) assays were performed to determine the effect of RAD51B on the proliferation of OC cells. RAD51B silencing inhibited cell proliferation and survival. Consistent with RAD51B-AS1, RAD51B downregulation also reduced metastasis (Figure 4G) and anoikis resistance (Figure 4H) in HO8910PM cells. In the soft agar assay, the anchor-independent growth of OC cells was significantly reduced after RAD51B knockdown (Figure S2B). RAD51B was positively associated with RAD51B-AS1 and exhibited pro-carcinogenic properties in OC.

3.5 RAD51B-AS1 mediates OC progression by regulating RAD51B expression

To further demonstrate that RAD51B-AS1 promotes cancer cell progression by interfering with RAD51B expression, rescue assays were conducted. It was revealed that si-RAD51B reversed the promotion of Bcl-2 expression following LV-RAD51B-AS1 overexpression (Figure. 5A). Furthermore, RAD51B-AS1 overexpression markedly increased OC cell growth (Figure 5B and C) and metastasis (Figure 5D), which was abolished by deleting RAD51B. Likewise, RAD51B knockdown reversed the promotion of anoikis resistance and anchor independent growth following RAD51B-AS1 upregulation (Figure 5E and S2C).

3.6 RAD51B-AS1 contributes to OC progression by regulating RAD51B expression in vivo.

To confirm whether RAD51B-AS1 affected the proliferation of OC cells through RAD51B in vivo, subcutaneous tumor mouse models were established. The results revealed that the tumor-promoting ability of the overexpressed group was significantly reduced compared with the control group, following an intratumoral injection of si-RAD51B (Figure 6A-C). Both the knockdown efficiency of si-RAD51B (Figure 6D) and the overexpression efficiency of LV-RAD51B-AS1 were verified (Figure 6E). RAD51B expression levels were increased following RAD51B-AS1 overexpression (Figure 6D), and the linear correlation between them was verified (Figure 6F). Immunohistochemistry confirmed that the RAD51B, Ki67 and Bcl-

2 proteins were significantly increased after RAD51B-AS1 overexpression and restored to their original levels in simultaneously overexpressed RAD51B-AS1 and RAD51B knocked-down cells (Figure 6G). Taken together, the results supported our in vitro findings and suggested that RAD51B-AS1 promoted OC through RAD51B *in vivo.*

3.7 High expression of RAD51B-AS1 is predictive of a poor prognosis

The correlation between RAD51B-AS1 expression levels and the clinical prognostic parameters of 49 patients with OC was evaluated. The results revealed that RAD51B-AS1 expression levels were positively correlated with poorer prognostic parameters, including FIGO stage and lymph node metastasis (Table 2). The results indicated that high expression of RAD51B-AS1 was a predictor of poor prognosis in patients with OC.

Table 2. Association between RAD51B-AS1 expression level and clinicopathological parameters of patients.

Variables	N	RAD51B-AS1 expression		p value
		low	high	
age□years□				0.228
≤50	12	5	7	
>50	37	7	30	
FIGO stage				**0.012***
I/II	10	6	4	
III/IV	39	6	33	
Lymph node metastasis				**0.044***
negative	23	9	14	
positive	26	3	23	
Serum CA125 (U/ml)				0.183
≤500	23	8	15	
>500	26	4	22	

* Bold values were presented as P□0.05

4. Discussion

An increasing number of studies have uncovered the indispensable role that lncRNAs play in the tumorigenesis and progression of various types of cancer [22-24]. For instance, MALAT1 has been

suggested to serve as a potential prognostic biomarker and therapeutic target in different types of cancer [9, 25-27]. Abnormal regulation of lncRNAs is tightly involved in the diagnosis and therapy of patients with cancer [28].

aslncRNAs are a class of transcripts that are complementary to their sense RNA strands of protein-coding genes, and have been shown to be widely expressed in a variety of tumors and cell lines [29-31]. aslncRNA exerts multiple functions and can act as positive or negative regulators of their homologous genes through cis or trans mechanisms [32]. However, the underlying mechanisms of aslncRNAs are complex. Depending on their localization, aslncRNAs can interact with DNA, RNA and protein to affect the gene expression process at the pre-transcriptional or post-transcriptional levels. This may involve mRNA splicing, stabilization of its complementary mRNA, mRNA localization and transport, and the initiation of sense-encoded proteins [33]. For instance, the lncRNA TPT1-AS1 promotes OC tumorigenesis and metastasis by promoting TPT1 expression and inducing the transcriptional activity of the TPT1 promoter [34]. Furthermore, lncRNA FOXC2-AS1 stabilizes the mRNA of its sense-cognate gene, FOXC2, to activate the Ca^{2+}-FAK signaling pathway and promote colorectal cancer progression [35]. GATA3-AS1 forms a DNA-RNA hybridization (R-loop) to enroll MLL methyltransferase at the gene site to regulate GATA3 expression [36]. However, no efficient and specific lncRNA has been identified or used for OC diagnosis or treatment, and its internal function and molecular mechanism have not been fully explored, meaning that further analysis is required.

In the present study, RAD51B-AS1 was confirmed to be expressed at high levels in OC tissues and markedly associated with unfavorable OC clinicopathological features, including III-IV FIGO stage and lymph node metastasis. Moreover, RAD51B-AS1 was revealed to markedly promote OC proliferation, migration and anoikis resistance *in vitro* and *in vivo*. Therefore, RAD51B-AS1 may play an oncogenic role in OC. RAD51B expression was positively correlated with RAD51B-AS1 expression and significantly elevated in patients with OC, which could indicate its role as a tumor promoting gene for OC. RAD51B is a paralog of the human gene RAD51. RAD51 protein levels have been reported to be a potential marker for prognosis and it has been reported to promote cell proliferation in pancreatic cancer [37]. Increased RAD51 expression levels has been associated with genome instability, tumor recurrence, tumor progression, and increased resistance to radiotherapy and chemotherapy in various types of cancer [38-40]. RAD51B also plays a crucial role in the regulation of these processes, and may therefore act as a candidate oncogene and biomarker for cancer detection and prognosis. Previously, RAD51B was been confirmed to exert pro-carcinogenic effects in certain types of cancer, was found to contribute to the tumorigenesis of gastric cancer, server as a potential biomarker for the early detection of gastric cancer and function as an indicator of poor prognosis [41]. Unfortunately, the clinical significance of RAD51B and its cellular functions in OC are not yet fully understood. The results of the present study revealed that RAD51B downregulation suppressed OC malignancy. These data suggested that RAD51B was a pro-oncogene in OC. However, the current study is limited by the sample size and the lack of determination of the underlying mechanisms of RAD51B in contributing to the progression of OC. Further studies are required

to understand the molecular mechanism through which RAD51B-AS1 regulates RAD51B, and through which RAD51B participants in the progression of OC.

These results may extend current knowledge about potential biomarkers and their prediction of overall survival in patients with OC, and guide therapeutic strategies for the disease. The results may also provide areas of study for determining the molecular mechanisms that underlie the development of OC, and provide new molecular markers and targets for the diagnosis and treatment of OC.

5. Conclusion

In summary, current study demonstrated that lncRNA RAD51B-AS1 promoted the malignant biological behavior of OC by activating RAD51B. The results may provide a potentially effective therapeutic target for OC.

Abbreviations

OC	Ovarian Cancer
LncRNA	Long non-coding RNA
RT-qPCR	Reverse transcription-quantitative PCR
cDNA	complementary DNA
CCK-8	Cell Counting Kit-8
FBS	fetal bovine serum
FISH	fluorescence in-situ hybridization
OS	overall survival
PFS	progression-free survival

Declarations

Ethics approval and consent to participate The study was conducted in accordance with the Declaration of Helsinki, and approved by Ethics Committee of Women's Hospital, School of Medicine, Zhejiang University (Approval Number: IRB-20210147-R) for studies involving humans. The animal study protocol was approved by Institutional Animal Care and Use Committee (Approval Number: IACUC-20200506-07).” for studies involving animals.

Consent for publication Not applicable

Availability of data and materials The data supporting the reported results of this study are included in the article.

Competing interests The authors declare no conflict of interest.

Authors' Contributions Conceptualization, W.L., X.X. and X.We.; methodology, X.We., C.W., Z.S. and J.Z.; validation, X.We., C.W. and S.T.; investigation, X.We. and Q.Y.; resources, X.C. and X.Wa; data curation, X.We., C.W. and S.T.; writing—original draft preparation, X.We.; writing—review and editing, W.L., J.X. and X.We.; supervision, J.X.; project administration, W.L. and J.X.; funding acquisition, W.L. All authors have read and agreed to the published version of the manuscript.

Funding: This research received no external funding

Acknowledgments: We thank all subjects who participated in this study and thank for the technical support by the Core facilities, Zhejiang University, School of medicine.

References

1. Sung H, Ferlay J, Siegel R L, Laversanne M, Soerjomataram I, Jemal A, Bray F. Global cancer statistics 2020: GLOBOCAN estimates of incidence and mortality worldwide for 36 cancers in 185 countries [J]. CA: a cancer journal for clinicians, 2021, 71(3):209-249.
2. Lheureux S, Gourley C, Vergote I, Oza A M. Epithelial ovarian cancer [J]. Lancet (London, England), 2019, 393(10177): 1240-53.
3. Xie W, Sun H, Li X, Lin F, Wang Z, Wang X. Ovarian cancer: epigenetics, drug resistance, and progression [J]. Cancer cell international, 2021, 21(1): 434.
4. Grossman D C, Curry S J, Owens D K, Barry M J, Davidson K W, Doubeni C A, Epling J W, Jr., Kemper A R, Krist A H, Kurth A E, et al. Screening for Ovarian Cancer: US Preventive Services Task Force Recommendation Statement [J]. Jama, 2018, 319(6): 588-94.
5. Bhan A, Soleimani M, Mandal S S. Long Noncoding RNA and Cancer: A New Paradigm [J]. Cancer research, 2017, 77(15): 3965-81.
6. Yang J, Peng S, Zhang K. LncRNA RP11-499E18.1 Inhibits Proliferation, Migration, and Epithelial-Mesenchymal Transition Process of Ovarian Cancer Cells by Dissociating PAK2-SOX2 Interaction [J]. Frontiers in cell and developmental biology, 2021, 9(697831.
7. Wu Y, Gu W, Han X, Jin Z. LncRNA PVT1 promotes the progression of ovarian cancer by activating TGF-β pathway via miR-148a-3p/AGO1 axis [J]. Journal of cellular and molecular medicine, 2021, 25(17): 8229-43.
8. Zhao L, Jiang L, Zhang M, Zhang Q, Guan Q, Li Y, He M, Zhang J, Wei M. NF-κB-activated SPRY4-IT1 promotes cancer cell metastasis by downregulating TCEB1 mRNA via Staufen1-mediated mRNA decay [J]. Oncogene, 2021, 40(30): 4919-29.
9. Pei C, Gong X, Zhang Y. LncRNA MALAT-1 promotes growth and metastasis of epithelial ovarian cancer via sponging microrna-22 [J]. American journal of translational research, 2020, 12(11): 6977-87.

10. Dai W, Tian C, Jin S. Effect of lncRNA ANRIL silencing on anoikis and cell cycle in human glioma via microRNA-203a [J]. OncoTargets and therapy, 2018, 11(5103-9.
11. Liang H, Yu T, Han Y, Jiang H, Wang C, You T, Zhao X, Shan H, Yang R, Yang L, et al. LncRNA PTAR promotes EMT and invasion-metastasis in serous ovarian cancer by competitively binding miR-101-3p to regulate ZEB1 expression [J]. Molecular cancer, 2018, 17(1): 119.
12. Qiu J J, Lin Y Y, Ding J X, Feng W W, Jin H Y, Hua K Q. Long non-coding RNA ANRIL predicts poor prognosis and promotes invasion/metastasis in serous ovarian cancer [J]. International journal of oncology, 2015, 46(6): 2497-505.
13. Shenhua X, Lijuan Q, Hanzhou N, Xinghao N, Chihong Z, Gu Z, Weifang D, Yongliang G. Establishment of a highly metastatic human ovarian cancer cell line (HO-8910PM) and its characterization [J]. Journal of experimental & clinical cancer research : CR, 1999, 18(2): 233-9.
14. Shen X, Wang C, Zhu H, Wang Y, Wang X, Cheng X, Ge W, Lu W. Exosome-mediated transfer of CD44 from high-metastatic ovarian cancer cells promotes migration and invasion of low-metastatic ovarian cancer cells [J]. Journal of ovarian research, 2021, 14(1): 38.
15. Liu X F, Thin K Z, Ming X L, Shuo L, Ping L, Man Z, Li N D, Tu J C. Small Nucleolar RNA Host Gene 18 Acts as a Tumor Suppressor and a Diagnostic Indicator in Hepatocellular Carcinoma [J]. Technology in cancer research & treatment, 2018, 17(1533033818794494.
16. Zheng R, Yao Q, Li X, Xu B. Long Noncoding Ribonucleic Acid SNHG18 Promotes Glioma Cell Motility via Disruption of α-Enolase Nucleocytoplasmic Transport [J]. Frontiers in genetics, 2019, 10(1140.
17. Huang L J, Shen Y, Bai J, Wang F X, Feng Y D, Chen H L, Peng Y, Zhang R, Li F M, Zhang P H, et al. High Expression Levels of Long Noncoding RNA Small Nucleolar RNA Host Gene 18 and Semaphorin 5A Indicate Poor Prognosis in Multiple Myeloma [J]. Acta haematologica, 2020, 143(3): 279-88.
18. Fan H, Yuan J, Li Y, Jia Y, Li J, Wang X, Li X. MKL1-induced lncRNA SNHG18 drives the growth and metastasis of non-small cell lung cancer via the miR-211-5p/BRD4 axis [J]. Cell death & disease, 2021, 12(1): 128.
19. Abdelmohsen K, Panda A, Kang M J, Xu J, Selimyan R, Yoon J H, Martindale J L, De S, Wood W H, 3rd, Becker K G, et al. Senescence-associated lncRNAs: senescence-associated long noncoding RNAs [J]. Aging cell, 2013, 12(5): 890-900.
20. Yuan D, Liu Y, Li M, Zhou H, Cao L, Zhang X, Li Y. Senescence associated long non-coding RNA 1 regulates cigarette smoke-induced senescence of type II alveolar epithelial cells through sirtuin-1 signaling [J]. The Journal of international medical research, 2021, 49(2): 300060520986049.
21. Lv Z, Sun L, Xu Q, Xing C, Yuan Y. Joint analysis of lncRNA m(6)A methylome and lncRNA/mRNA expression profiles in gastric cancer [J]. Cancer cell international, 2020, 20(464.
22. Dang W, Cao P, Yan Q, Yang L, Wang Y, Yang J, Xin S, Zhang J, Li J, Long S, et al. IGFBP7-AS1 is a p53-responsive long noncoding RNA downregulated by Epstein-Barr virus that contributes to viral tumorigenesis [J]. Cancer letters, 2021, 523:135-147.
23. Luo C, Lin K, Hu C, Zhu X, Zhu J, Zhu Z. LINC01094 promotes pancreatic cancer progression by sponging miR-577 to regulate LIN28B expression and the PI3K/AKT pathway [J]. Molecular therapy

Nucleic acids, 2021, 26(523-35.

24. Yin H, Chen L, Piao S, Wang Y, Li Z, Lin Y, Tang X, Zhang H, Zhang H, Wang X. M6A RNA methylation-mediated RMRP stability renders proliferation and progression of non-small cell lung cancer through regulating TGFBR1/SMAD2/SMAD3 pathway [J]. Cell death and differentiation, 2021,
25. Gordon M A, Babbs B, Cochrane D R, Bitler B G, Richer J K. The long non-coding RNA MALAT1 promotes ovarian cancer progression by regulating RBFOX2-mediated alternative splicing [J]. Molecular carcinogenesis, 2019, 58(2): 196-205.
26. Feng C, Zhao Y, Li Y, Zhang T, Ma Y, Liu Y. LncRNA MALAT1 Promotes Lung Cancer Proliferation and Gefitinib Resistance by Acting as a miR-200a Sponge [J]. Archivos de bronconeumologia, 2019, 55(12): 627-33.
27. Li C, Cui Y, Liu L F, Ren W B, Li Q Q, Zhou X, Li Y L, Li Y, Bai X Y, Zu X B. High Expression of Long Noncoding RNA MALAT1 Indicates a Poor Prognosis and Promotes Clinical Progression and Metastasis in Bladder Cancer [J]. Clinical genitourinary cancer, 2017, 15(5): 570-6.
28. Huarte M. The emerging role of lncRNAs in cancer [J]. Nature medicine, 2015, 21(11): 1253-61.
29. Faghihi M A, Wahlestedt C. Regulatory roles of natural antisense transcripts [J]. Nature reviews Molecular cell biology, 2009, 10(9): 637-43.
30. Katayama S, Tomaru Y, Kasukawa T, Waki K, Nakanishi M, Nakamura M, Nishida H, Yap C C, Suzuki M, Kawai J, et al. Antisense transcription in the mammalian transcriptome [J]. Science (New York, NY), 2005, 309(5740): 1564-6.
31. Deng S J, Chen H Y, Zeng Z, Deng S, Zhu S, Ye Z, He C, Liu M L, Huang K, Zhong J X, et al. Nutrient Stress-Dysregulated Antisense lncRNA GLS-AS Impairs GLS-Mediated Metabolism and Represses Pancreatic Cancer Progression [J]. Cancer research, 2019, 79(7): 1398-412.
32. Cui X Y, Zhan J K, Liu Y S. Roles and functions of antisense lncRNA in vascular aging [J]. Ageing research reviews, 2021, 101480.
33. Statello L, Guo C J, Chen L L, Huarte M. Gene regulation by long non-coding RNAs and its biological functions [J]. Nature reviews Molecular cell biology, 2021, 22(2): 96-118.
34. Wu W, Gao H, Li X, Zhu Y, Peng S, Yu J, Zhan G, Wang J, Liu N, Guo X. LncRNA TPT1-AS1 promotes tumorigenesis and metastasis in epithelial ovarian cancer by inducing TPT1 expression [J]. Cancer science, 2019, 110(5): 1587-98.
35. Zhang C L, Zhu K P, Ma X L. Antisense lncRNA FOXC2-AS1 promotes doxorubicin resistance in osteosarcoma by increasing the expression of FOXC2 [J]. Cancer letters, 2017, 396(66-75.
36. Gibbons H R, Shaginurova G, Kim L C, Chapman N, Spurlock C F, 3rd, Aune T M. Divergent lncRNA GATA3-AS1 Regulates GATA3 Transcription in T-Helper 2 Cells [J]. Frontiers in immunology, 2018, 9(2512.
37. Zhang X, Ma N, Yao W, Li S, Ren Z. RAD51 is a potential marker for prognosis and regulates cell proliferation in pancreatic cancer [J]. Cancer cell international, 2019, 19(356.

38. Huang J, Luo H L, Pan H, Qiu C, Hao T F, Zhu Z M. Interaction between RAD51 and MCM Complex Is Essential for RAD51 Foci Forming in Colon Cancer HCT116 Cells [J]. Biochemistry Biokhimiia, 2018, 83(1): 69-75.
39. Alshareeda A T, Negm O H, Aleskandarany M A, Green A R, Nolan C, Tighhe P J, Madhusudan S, Ellis I O, Rakha E A. Clinical and biological significance of RAD51 expression in breast cancer: a key DNA damage response protein [J]. Breast cancer research and treatment, 2016, 159(1): 41-53.
40. Chen Q, Cai D, Li M, Wu X. The homologous recombination protein RAD51 is a promising therapeutic target for cervical carcinoma [J]. Oncology reports, 2017, 38(2): 767-74.
41. Cheng Y, Yang B, Xi Y, Chen X. RAD51B as a potential biomarker for early detection and poor prognostic evaluation contributes to tumorigenesis of gastric cancer [J]. Tumour biology : the journal of the International Society for Oncodevelopmental Biology and Medicine, 2016, 37(11): 14969-78.

Figures

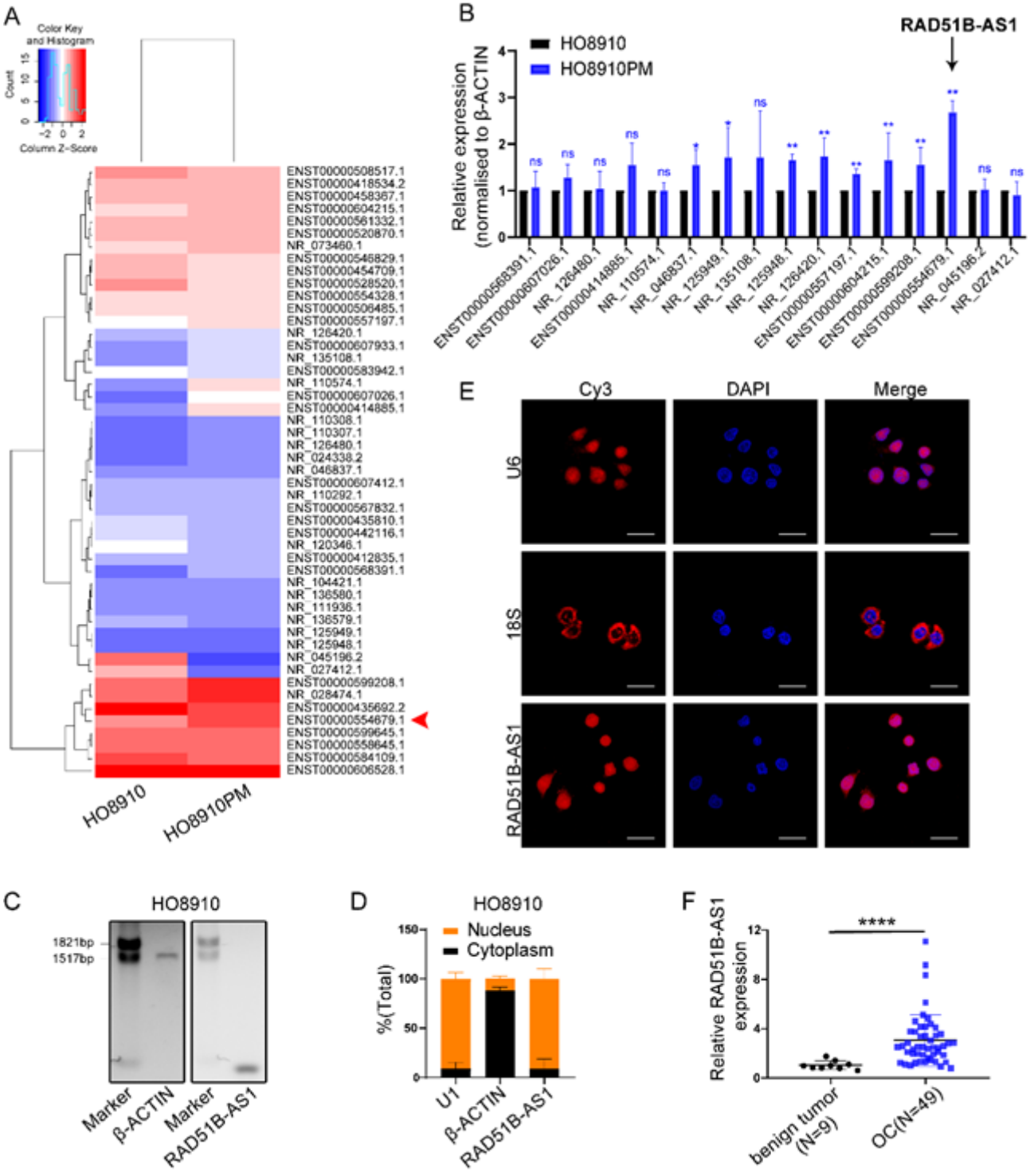

Figure 1

Identification and characterization of RAD51B-AS1. (**A**) Heatmap of differentially expressed lncRNAs between HO8910 and HO8910PM[$\log_2$(fold change)≥2 or ≤-2，P＜0.05]. The red arrow indicates lncRNA RAD51B-AS1. (**B**) The expressions of sixteen selected lncRNAs were detected by RT-qPCR in HO8910 and HO8910PM cells. Results shown are means ± SD(n≥3), *p < 0.05. (**C**) The validation of RAD51B-AS1 by Northern Blotting. (**D**) Subcellular fractionation detection showed the location of RAD51B-AS1. Results shown are means ± SD for three separate experiments. (**E**) FISH assay showed the location of RAD51B-

AS1 with U6 and 18S as internal reference. Scale bar, 20μm. (**F**) The expression of RAD51B-AS1 in benign ovarian tumors and ovarian cancer tissues. Results were shown as means ± SD. ****p < 0.0001.

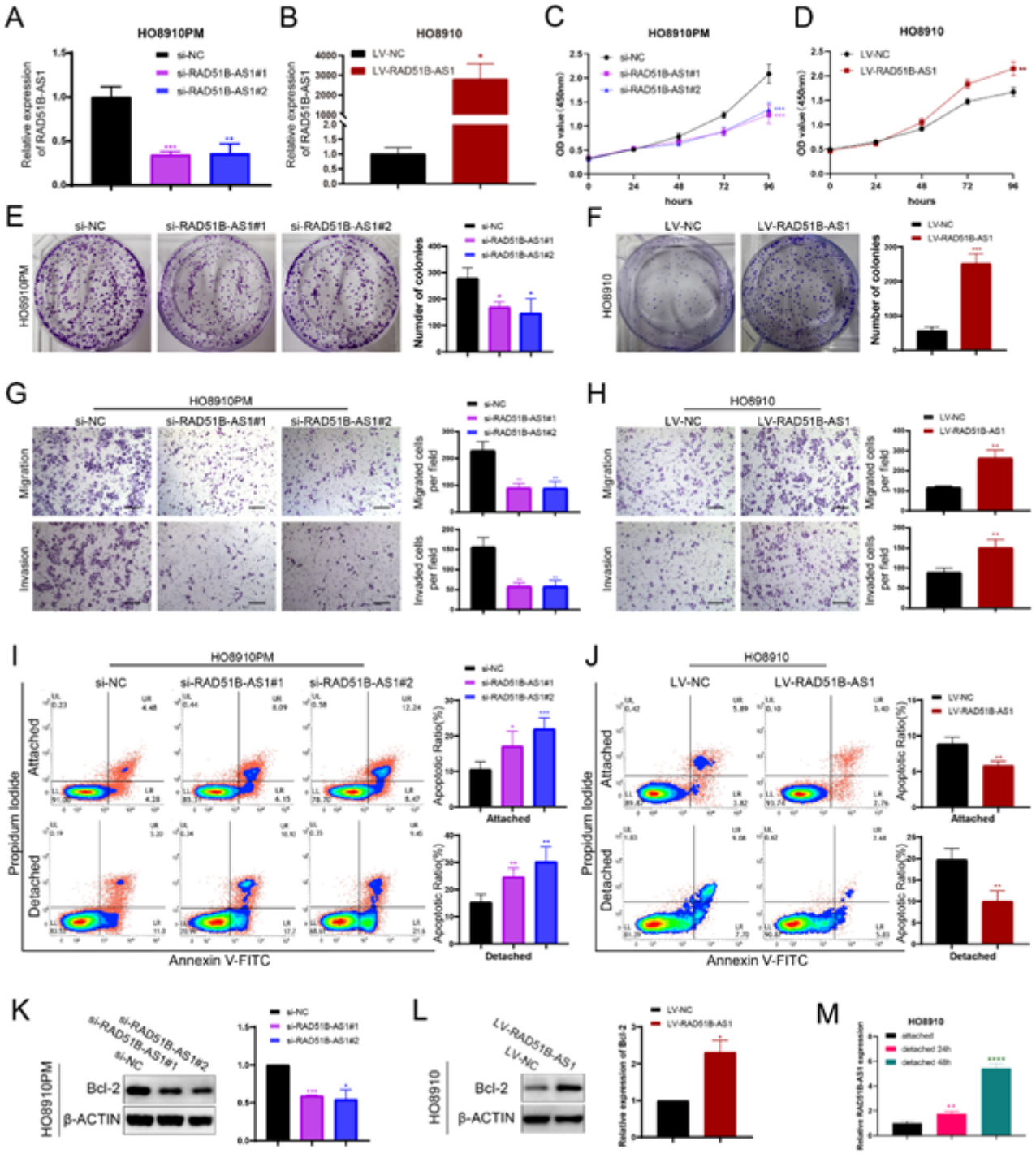

Figure 2

LncRNA RAD51B-AS1 enhances growth and metastasis and anoikis resistance in ovarian cancer cells. (**A**) Verification of knockdown efficiency of two specific siRNAs targeting RAD51B-AS1 in HO8910PM cells using RT-qPCR analysis. (**B**) Verification of efficiency of lentivirus overexpression in HO8910 cells using RT-qPCR analysis. (**C, D**) CCK-8 assays showed proliferation of HO8910 and HO8910PM cells treated with knockdown(**C**) or overexpression(**D**) of RAD51B-AS1. (**E, F**) Representative images of colony-

formation assays for the survival ability in HO8910PM and HO8910 cells with RAD51B-AS1 down-regulation(**E**) and up-regulation(**F**) are shown in left panels, respectively. Statistics of colony numbers per well are shown in right graphs. (**G,H**) Transwell assays demonstrated the migration and invasion ability after knockdown(**G**) or overexpression(**H**) of RAD51B-AS1. Scale bar, 100μm. (**I, J**) Apoptotic rates after knocking down(**I**) or overexpressing(**J**) RAD51B-AS1 when cells were attached or detached. (**K, L**) Western blotting assays showed expression of Bcl-2 protein while dysregulation of RAD51B-AS1. (**M**) The expression level of RAD51B-AS1 was detected by RT-qPCR in HO8910 cells at 24h and 48h after induced suspension. Results were shown as means ± SD, n≥3 ,*p<0.05, **p<0.01, ***p<0.001,****p<0.0001

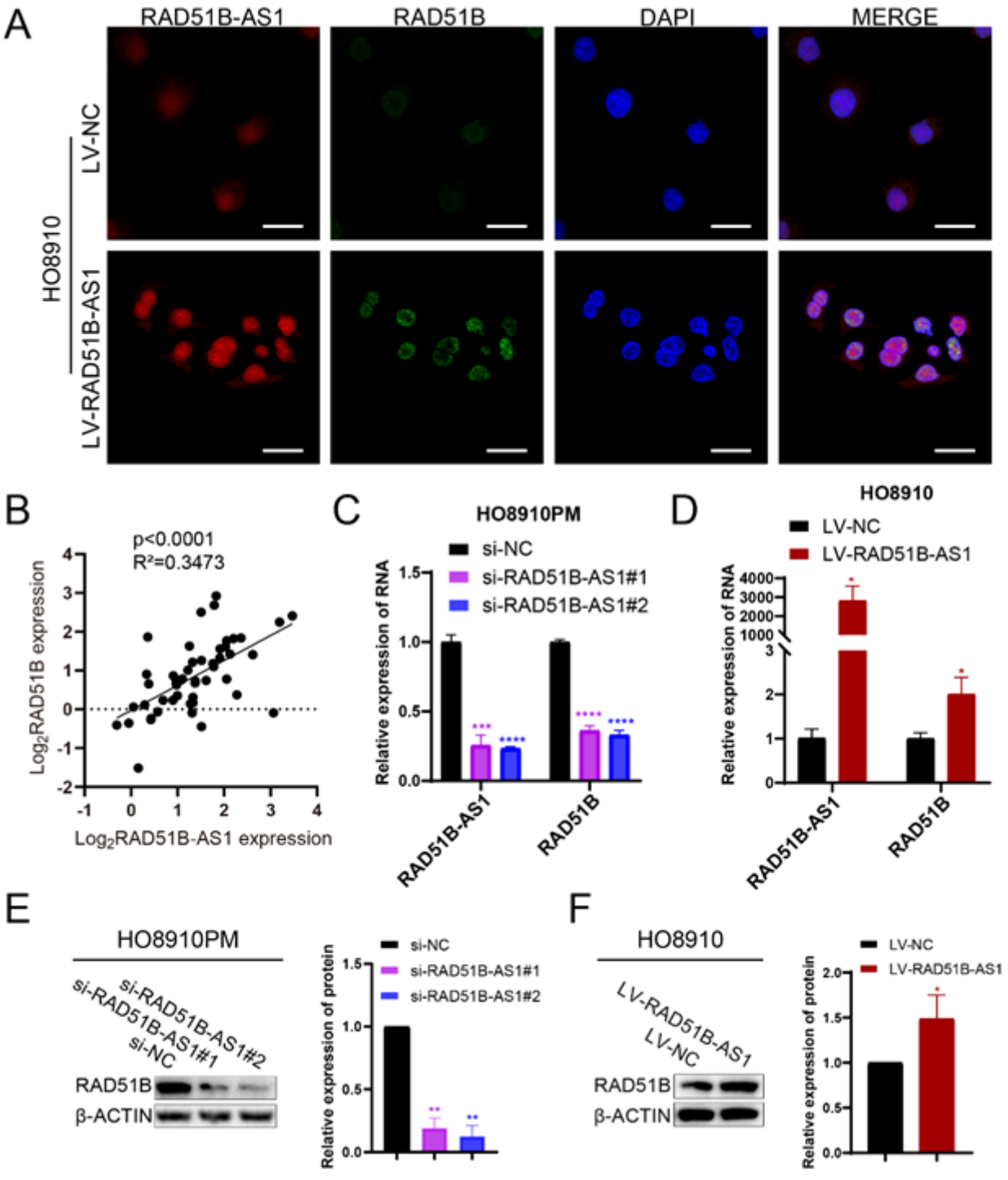

Figure 3

RAD51B-AS1 positively regulates RAD51B. (**A**) FISH and immunofluorescence co-localization showed that RAD51B-AS1 and RAD51B co-localized in the nucleus. Scale bar, 20μm. (**B**) The linear correlation between RAD51B-AS1 and RAD51B in 49 cases of OC using RT-qPCR analysis. (**C,D**) RT-qPCR showed mRNA level of RAD51B after silencing(**C**) or overexpression(**D**) of RAD51B-AS1 (**E,F**)Western blotting analysis showed protein level of RAD51B after knockdown(**E**) or overexpression(**F**) of RAD51B-AS1. Results were shown as means ± SD for three separate experiments. *p＜0.05，**p＜0.01，***p＜0.001, ****p＜0.0001.

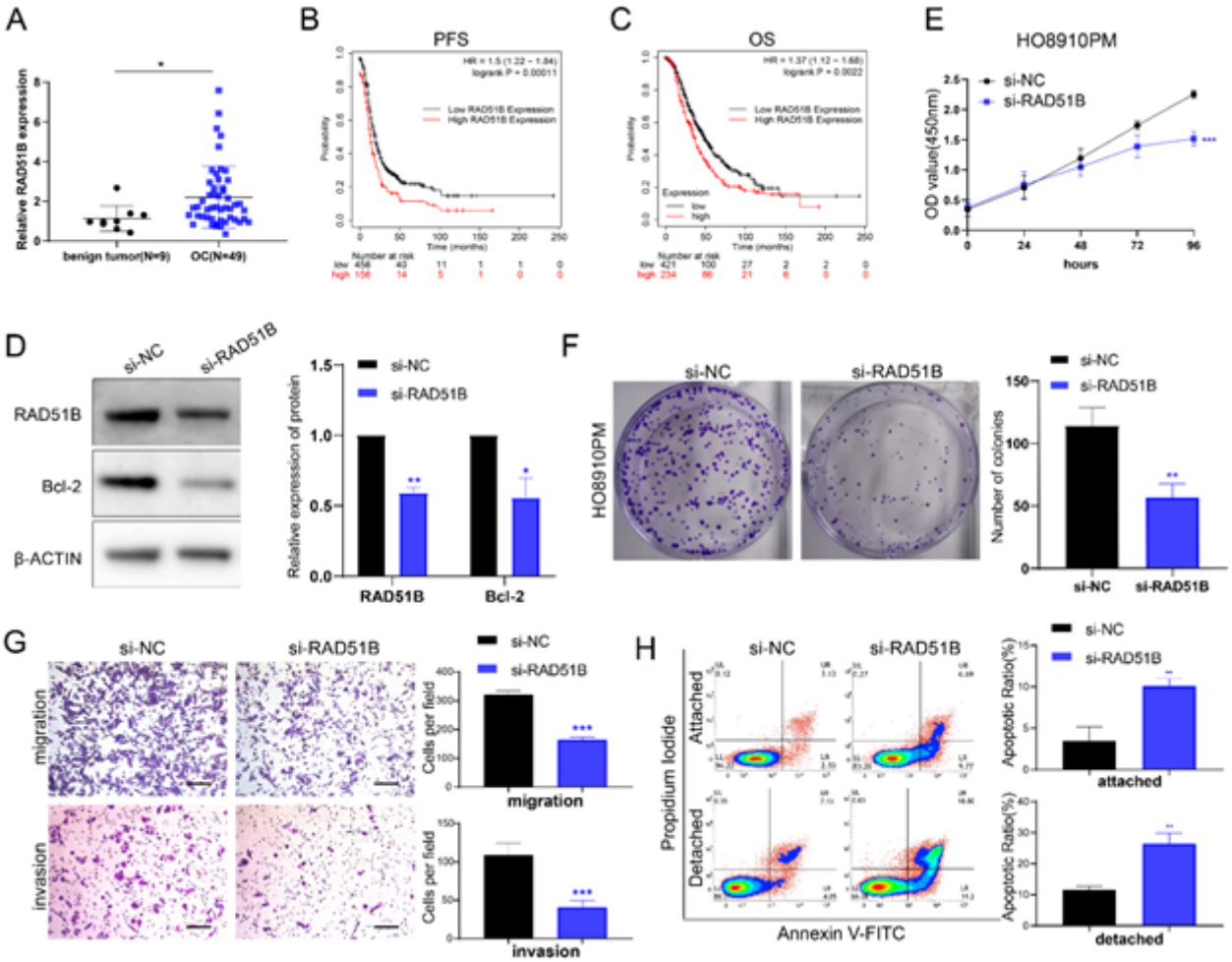

Figure 4

RAD51B promotes the malignant biological behavior of ovarian cancer. (**A**) Comparison of RAD51B expression in benign ovarian tumors and ovarian cancer tissues using RT-qPCR.(**B,C**) Kaplan-Meier analysis of progression-free survival(**B**) and overall survival(**C**) of OC patients based on the Kaplan-Meier Plotter online database (Affymetrix ID: 1554496_at; all, P<0.05) (**D**) Bcl-2 expression are showed after RAD51B knockdown using western blotting analysis.(**E**) CCK-8 assays showed cell growth ability after RAD51B knockdown.(**F**) Colony formation assays showed HO8910PM cells colony formation ability.(**G**) Transwell assays showed cells migration and invasion when RAD51B was knockdown. Scale bar, 100μm.

(**H**) Apoptotic rate after knocking down RAD51B when cells were attached or detached. Results were shown as means ± SD for three separate experiments. *p<0.05;**p<0.01;***p<0.001

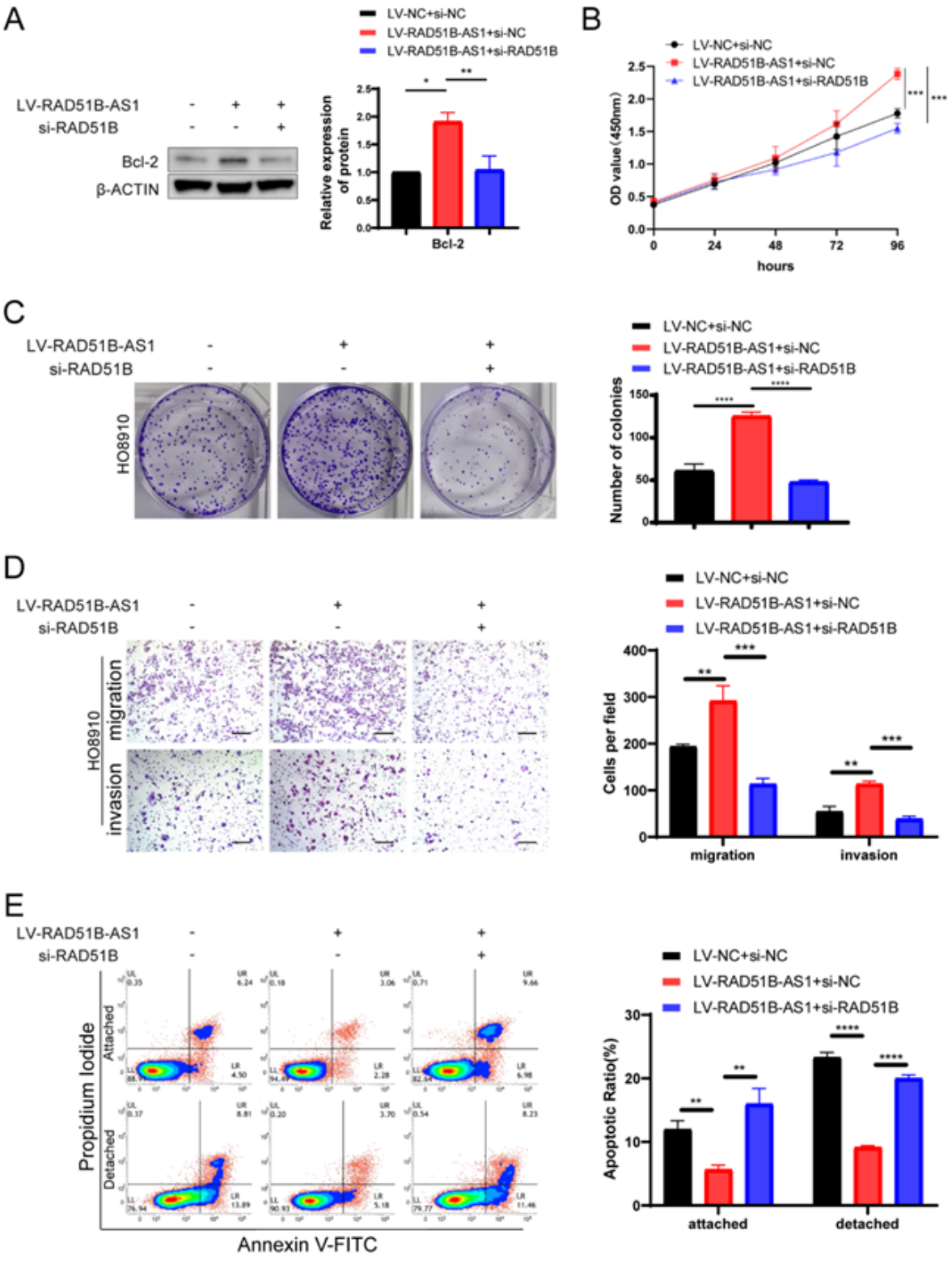

Figure 5

RAD51B-AS1 mediates OC progression by regulating RAD51B expression. (**A**) western blotting assays were used to verify the expression levels of Bcl-2. (**B**) CCK-8 assays were used to observe the growth of

cells. (**C**) The cell colony formation and viability were observed by plate colony formation experiment. (**D**) Cell migration and invasion ability were observed by Trans-well assay. Scale bar, 100μm. (**E**) Apoptosis rate of adherent and suspended cells was observed by flow cytometry. Results were shown as means ± SD for three separate experiments. *p<0.05 **p<0.01 ***p<0.001 ****p<0.0001

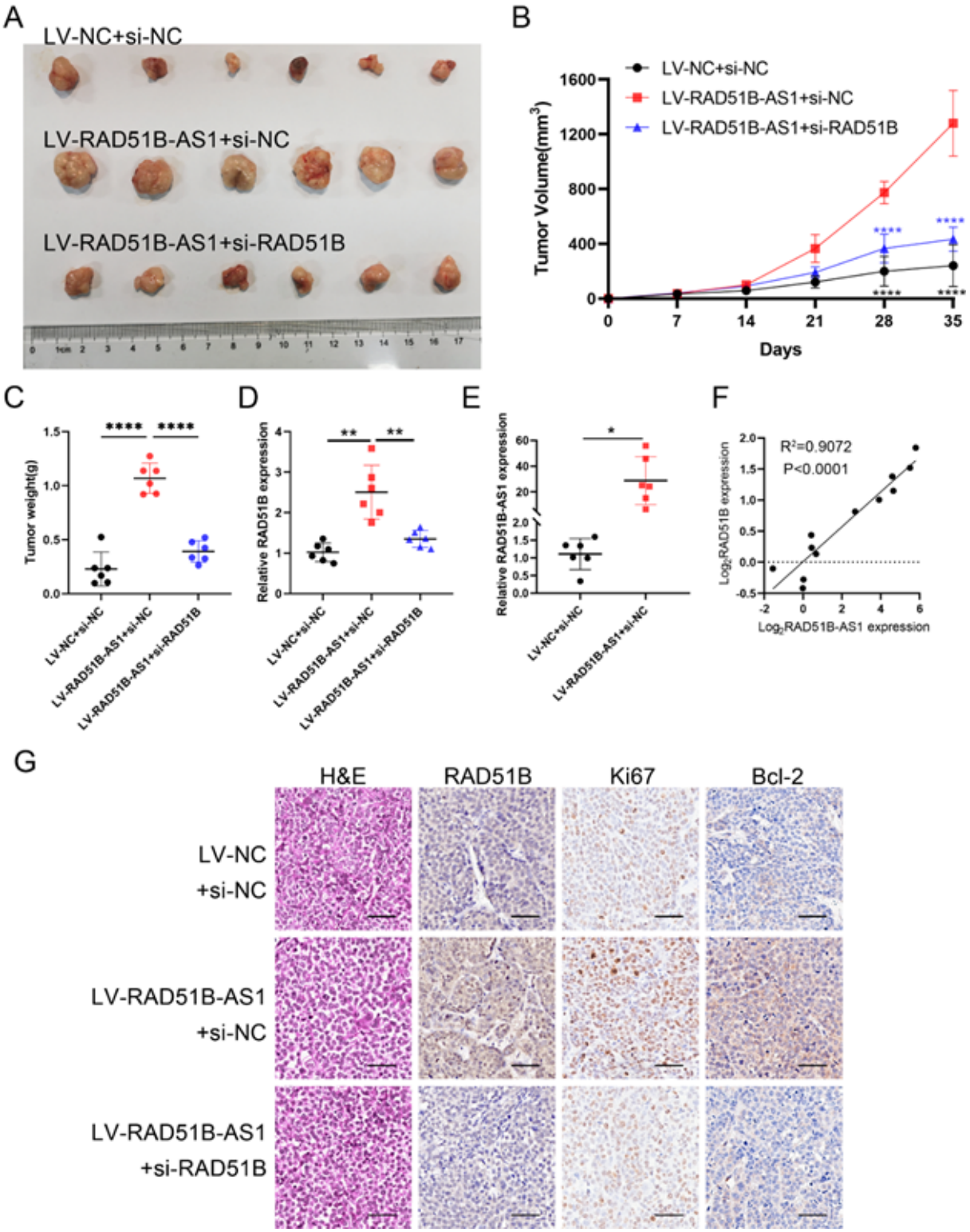

Figure 6

RAD51B-AS1 contributes to progression of ovarian cancer by regulating RAD51B expression in vivo. (**A**) Final volume of subcutaneous neoplasm in nude mice. (**B**) The volume growth curve of subcutaneous tumor in nude mice.(**C**) Weight of subcutaneous neoplasm in nude mice.(**D**) The expression of RAD51B in the tumor was detected by RT-qPCR.(**E**) The expression of RAD51B-AS1 in the tumor was detected by RT-qPCR.(**F**) Analysis of linear relationship between lncRNA RAD51B-AS1 and RAD51B mRNA.(**G**) IHC analysis of RAD51B,Ki67 and Bcl-2. Scale bar, 50μm. Results were shown as means ± SD for three separate experiments. *p□0.05□**p□0.01□***p□0.001□****p□0.0001

Supplementary Files

This is a list of supplementary files associated with this preprint. Click to download.

- supplementarydata.docx
- Supplementaryfigure1.tif
- Supplementaryfigure2.tif